

ANALYTICAL REPORT

[Ref.: AAR0955.D / 8 May 2018]



The Jewish Family, 1912

Natalia Goncharova

Collection Museum Ludwig, Cologne, Inv. ML 1369

Art Analysis & Research Inc.
Ground Floor West, 162-164 Abbey Street, London SE1 2AN
T: +44 (0) 20 7064 1433
VAT Reg. No. 252 4541 22



Summary

A painting on canvas by Natalia Goncharova, *The Jewish Family*, with a proposed date of creation of 1912 (it is signed but undated), belonging to the Museum Ludwig (ML 1369) was examined and analysed by Art Analysis & Research, Ltd. in cooperation with the Museum, and funded through a grant from the charity The Russian Avant Garde Research Project (RARP). This artwork was assessed as part of a group of fourteen well-provenanced paintings by the Russian artist couple Goncharova and Mikhail Larionov, held in the collection of the Museum Ludwig. The goal set for this research was to investigate these paintings in order to characterise similarities and differences, with the goals of 1) providing detailed studies of specific paintings, 2) providing wider information on the artists' methods, 3) defining a blueprint for promising methodologies to develop further on other works by these artists and applying such information in support of a *catalogue raisonné*, and 4) creating the foundation for applying similar methodologies and techniques to other artists of the genre. To this end, each of the paintings are described in individual reports (as here) accompanied by a summary report under separate cover. The results of the program of examination, material analysis and technical imaging will be set out herein.



Contents

Summary	2
Tables, Figures and Plates.....	4
A. Introduction.....	6
B. Examination, imaging and analysis of the images	7
B.1 Methodology	7
B.2 General observations	7
B.3 Imaging.....	8
B.3.i Photography with ultraviolet illumination	8
B.3.ii Surface conformation	8
B.3.iii Short-wave infrared (SWIR).....	9
B.3.iv X-radiography and weave analysis	9
C. Sampling and analysis	10
C.1 Introduction	10
C.2 Support	11
C.3 Radiocarbon dating.....	11
C.4 Ground.....	12
C.5 Underdrawing.....	12
C.6 Paint layers: Pigments	12
C.7 Paint layers: Binding media	12
C.8 Stratigraphy	13
D. Discussion of the findings.....	13
D.1 Support, ground and preparatory work	13
D.1.i The support	13
D.1.ii Priming.....	14
D.1.iii Underdrawing	14
D.2 Paint, pigments and binding media	15
D.2.i General observations.....	15
D.2.ii Paint: pigment and binding medium	16
D.2.iii Materials analysis and implications for dating	17
E. Conclusions	17
F. Acknowledgements.....	18
G. Appendices.....	19

App.1 Sampling and sample preparation	19
App.1.i Sampling	19
App.1.ii Cross-sectional analysis	20
App.2 Materials analysis summary results	21
App.2.i SEM-EDX, Raman microscopy and PLM analysis	22
App.2.ii Fourier Transform Infrared Spectroscopy-Attenuated Total Reflectance (FTIR-ATR)	24
App.2.iii Gas Chromatography Mass Spectrometry (GCMS) Analysis	25
App.2.iv Fibre Identification of the Canvas.....	26
App.2.v Radiocarbon measurement	26
App.3 Imaging methods	27
App.4 Plates	28
App.5 Cross-sections	46

Tables, Figures and Plates

Table App.1.i Samples taken for analysis.....	19
Table App.2.i Analytical results SEM-EDX, Raman Microscopy and PLM	22
Table App.2.ii Summary results from FTIR	24
Table App.2.iii Summary results from GCMS	25
Table App.2.iv Canvas fibre identification, Sample [18]	26
Table App.2.v.i Radiocarbon measurement.....	27
Figure App.2.v.ii Radiocarbon determination.	27
Plate 1. Natalia Goncharova, The Jewish Family, 1912, collection Museum Ludwig: Inv. Nr. ML 1369. Recto, visible light.	28
Plate 2. Natalia Goncharova, The Jewish Family, 1912, collection Museum Ludwig: Inv. Nr. ML 1369. Recto, UV light.	29
Plate 3. Natalia Goncharova, The Jewish Family, 1912, collection Museum Ludwig: Inv. Nr. ML 1369. Recto, raking light.....	30
Plate 4.a Natalia Goncharova, The Jewish Family, 1912, collection Museum Ludwig: Inv. Nr. ML 1369. Recto, 3D laser scan.....	31
Plate 4.b Recto, 3D laser scan, detail. Figure of the standing woman, face, lace collar, torso.....	32
Plate 5. Natalia Goncharova, The Jewish Family, 1912, collection Museum Ludwig: Inv. Nr. ML 1369. Verso, visible light.	33
Plate 6. Natalia Goncharova, The Jewish Family, 1912, collection Museum Ludwig: Inv. Nr. ML 1369. Verso, UV light.	34
Plate 7. Natalia Goncharova, The Jewish Family, 1912, collection Museum Ludwig: Inv. Nr. ML 1369. Recto, SWIR image.....	35
Plate 8. Natalia Goncharova, The Jewish Family, 1912, collection Museum Ludwig: Inv. Nr. ML 1369. Recto, SWIR image, detail.....	36

Plate 9.a Natalia Goncharova, The Jewish Family, 1912, collection Museum Ludwig: Inv. Nr. ML 1369. X-ray image.....	37
Plate 9.b. X-ray image, before digital compensation for the stretcher bars.....	38
Plate 10.a Maps showing variation in canvas thread angle.....	38
Plate 10.b Histogram of vertical thread count readings.....	39
Plate 10.c Histogram of horizontal thread count readings.....	39
Plate 10.d Table of thread count data (threads per centimetre)	39
Plate 11.a Detail of canvas, verso.....	40
Plate 11.b Detail of canvas, left tacking margin, showing selvedge.....	40
Plate 11.c Detail of canvas, right tacking margin.....	40
Plate 12.a Detail of canvas, bottom tacking margin, showing the former turn over edge of the canvas.....	41
Plate 12.b Detail of canvas, left tacking margin, showing loss of white ground.....	41
Plate 12.c (Below) macro detail of the zinc white-based priming on the canvas.....	41
Plate 13.a Detail, recto, showing fibrous surface of the canvas and underdrawing.....	42
Plate 13.b Detail, recto, showing canvas and underdrawing.....	42
Plate 13.c Detail, recto, showing the exposed canvas with apparent loss of priming.....	42
Plate 14.a Microscope detail, showing the large particle size of the pigments.....	43
The paint surface has a flattened aspect.....	43
Plate 14.b Detail, recto, showing brushwork of the leaves.....	43
Plate 14.c Detail, recto, showing application of paint with a palette knife.....	43
Plate 15. Detail, a.) (above) X-ray.....	44
Plate 16. Image showing approximate location of samples taken for materials analysis.....	45
Plate 17. Cross section, Sample [3].....	46
Plate 18. Cross section, Sample [9].....	46

A. Introduction

The painting known as *The Jewish Family* (**Plate 1**) by the artist Natalia Goncharova (1881-1962), a work on canvas measuring 1585 mm high by 1320 mm wide, is now part of the collection of the Museum Ludwig, Cologne (Inv. ML 1369). It is signed, though undated; a date of 1912 has been proposed for its creation. It has been examined as part of a larger technical study of fourteen paintings by Goncharova and Mikhail Larionov in the Museum Ludwig, as part of a project funded through a grant from the charity the Russian Avant Garde Research Project (RARP). The project goal has been to generate detailed technical profiles on authentic paintings by Goncharova and Larionov to expand the data available for art historical study and technical characterization of their work¹; consequently, fourteen well-provenanced paintings by the Russian artist couple held in the collection of the Museum Ludwig were thoroughly examined and analysed². The short-term goal of the project was to define a blueprint for promising routes of research to develop further on other works by these artists and with a long-term goal of contributing such information to support a technical *catalogue raisonné*; these recommendations are laid out in a summary report³.

The information in this report therefore provides a detailed technical and material account of the painting. In addition, this material is considered in light of the conservation history and provenance information relating to the painting, held by the Museum Ludwig; the supplementary reports produced by Verena Franken in the course of her work on the RARP project summarises this material⁴. Some of the information concerning examination of the paintings has been included here, as relevant, as are a representative selection of the extensive documentation photographs she made.

The structure of this report is as follows. First, the primary findings of the visual examination and technical imaging will be described in **Section B**.

Materials analysis on micro-samples taken for pigment and binding medium identification and cross-sections is described in **Section C**.

¹ There is limited specific information available. This includes: Rioux, J.-P.; Aitken, G.; Duval, A. 'Étude en laboratoire des peintures de Gontcharova et Larionov', pp. 220-223. In: *Nathalie Gontcharova, Michel Larionov* [exh. cat.], Paris (1995). Rioux, J.-P.; Aitken, G.; Duval, A. 'Matériaux et techniques des peintures de Nathalie S. Gontcharova et Michel F. Larionov du Musée national d'art moderne', *Techné* 8 (1998) 7-32. Gallone, A. 'Œuvres de Michel Larionov et Nathalie Gontcharova: Analyse de la Couleur', *Le dessin sous-jacent la technologie dans la peinture: Colloque XI 14-16 septembre 1995*, R. Van Schoute and H. Verougstraete (eds), Louvain-la-Neuve (1997) pp. 137-141, Pl. 74-76.

² These include: Natalia Goncharova: *Paysage de Tiraspol (Tiraspol Landscape)*, 1905, ML 01483; *Rusalka*, 1908, ML 1304; *Still Life with Tiger Skin*, 1908, ML 1305; *The Jewish Family*, 1912, ML 1369; *The Orange Seller*, 1916, ML 1484; *Portrait of Larionov*, 1913, ML 1319.

Mikhail Larionov, *Still Life with Coffee Pot*, c. 1906, ML 01486; *Still Life*, c. 1907/1912, ML 1487; *Still Life with a Crayfish (Nature morte à l'écrevisse)*, c. 1907, ML 1331; *Portrait of a Man (Anton Beswal)*, c. 1910, ML 1306; *Rayonism, Red and Blue (Beach)*, 1911, ML 1333; *Saucisson et maquereau rayonists (Rayonistic Sausage and Mackerel)*, 1912, ML 1307; *Venus*, 1912, ML 1332; *Rayonistic Composition*, inscribed 1916, ML/Z 211/134.

³ *Summary Report of the RARP Goncharova/Larionov Project, with the Museum Ludwig*, Art Analysis & Research Inc. (2017).

⁴ See reports: *AAR0955.D ML 1369 Conservation*, Franken, V. 'Report on the examination of the painting *The Jewish Family* (1912) by Natalia Goncharova' (2017a) and *AAR0955.D ML 1369 Archives*, Franken, V. 'Report on the content of the Museum Ludwig archives, concerning the painting *The Jewish Family* (1912) by Natalia Goncharova' (2017b).

Inferences drawn regarding the painting on the basis of these investigations will be discussed in **Section D**.

The methodologies and protocols used in each case may be found described in the general **Protocols** supplement, appended to this series of reports.

B. Examination, imaging and analysis of the images

B.1 Methodology

The painting was initially examined visually under normal lighting conditions and with ultraviolet light (UV), then with a stereo binocular microscope.

A range of technical imaging techniques were also employed (**Appendix 3**), generating a variety of images and imaging datasets⁵. These are presented as follows:

- High-resolution visible colour (**Plates 1, 5**);
- UV luminescence (**Plates 2, 6**);
- Oblique illumination (**Plate 3**);
- 3D laser surface scanning (**Plate 4**);
- Short-wave infrared (SWIR), 1600-2500nm (**Plates 7, 8**);
- X-radiography (**Plate 9**).

Additionally, weave analysis (including thread counting) was conducted on the basis of the X-radiograph (**Plates 10.a-d**). Some exemplar images recorded as part of the surface microscopy and macrophotography are also reproduced here (**Plates 11-15**).

The imaging revealed a range of aspects regarding the use of materials, structure and technique of production of the painting that are complementary to the visual observations made. Consequently, specific observation will be made to each in this section regarding the interpretation of these specific forms of analysis, while a summary overview in the context of the painting technique is presented in **Section D**, below.

B.2 General observations

The painting is executed on a medium weight canvas, which has not been lined. Its tacking margins are present along both the right and left sides, so that both the recto and the verso of the artwork could be studied. The stretcher is not original, as the work has been re-stretched onto a newer secondary support, a stretcher with two crossbars (horizontal and vertical) and 10 keys (**Plate 5**). Despite problems with drying crack and brittleness, the painting is in good condition, with

⁵ Additionally, a visible-NIR multispectral dataset was collected to examine its suitability for study of paintings of Goncharova and Larionov. This has not been otherwise reproduced or further analysed here but is available for study in the future.

conservation interventions limited to minor, localised retouching and consolidation of the flaking areas. The painting is not varnished.

B.3 Imaging

Each form of imaging offers different types of insight into the various material aspects of the painting. The most relevant are introduced, in brief, here.

B.3.i Photography with ultraviolet illumination

Excitation by ultraviolet (UV) light can induce luminescence⁶ in some materials, commonly seen as a weak re-emission of light in the visible region. Many natural varnishes have this property, emitting a characteristic weak greenish luminescence. While some pigments (notably zinc white and certain ‘lake’ pigments) are also active in this way, paints otherwise often do not luminesce. Because of the luminescence of varnishes, which are typically applied as a continuous coating across the surface of a painting, this can provide a means of determining if any disturbance has occurred, such as partial cleaning of the surface or addition of later restoration, where the changes show in contrast to the luminescent areas. Consequently, UV light is commonly used to reveal the presence of retouching. When paintings are not varnished, as is the case here, differences between the colour of the luminescence of the different paints and any added retouching paints may also indicate later stages of intervention (as here; **Protocol 3.2** and **Plate 2**).

In the UV image of this work, no evidence for a varnish is visible. Much of the retouching is visible under UV illumination and may be seen to be concentrated along the edges of the work. Apart from the zinc white, which is visible as quite a bright, bluish green tone, no strong luminescence was noted from any of the original paints.

B.3.ii Surface conformation

Two techniques for examination of the surface structure of the painting were used: photography under oblique illumination and 3D laser scanning. While the former may be the more familiar of the two as a physical examination technique, both essentially provide a means of elucidating paint texture and object deformations, either by recording shadowing, or through direct measurement of surface height. Of the two, 3D laser scanning offers important advantages in terms of being more replicable in the future (to support longer-term conservation assessments for example) and as a numerical dataset that can be studied visually and algorithmically for diagnostic features of technique. Imaging of the painting using oblique illumination, as well as 3D laser surface scanning (see **Protocol 3.3**), served to reveal two kinds of textural features that are particularly evident in this painting. The most visually

⁶ Commonly referred to as ‘UV fluorescence’, the word *luminescence* is used here as a broader term that may encompass not only fluorescence phenomena (prompt re-emission of light), but also phosphorescence (slow re-emission of light due to transition via forbidden quantum states). In both cases emission is typically at longer wavelengths than the excitation; here, the excitation is in the UV to blue part of the spectrum (hence ‘UV’; in practice, so-called UV-A) and emission in the visible region.

dominant is the narrow, horizontal cracking that is prominent in the most thickly painted areas, while being effectively absent for more thinly painted regions (**Plates 4.a, 4.b**).

A strong crease is visible in the middle of the painting, running vertically from top to bottom. In addition, what appear to be lesser creases appear to run horizontally across the canvas – a number of these may be discerned. The clearest are those towards the lowermost edge; further up, it is not clear if these features pass fully through the width of the canvas. This type of deformation is likewise reflected in the thread density map, which provides a useful comparison reference (see section **B.3.iv**, below, and **Plate 10.a**).

Other characteristics of the canvas, such as the distribution of slub threads, may also be seen. As the cracking texture is horizontally oriented, the inclusion of slub threads in the vertical direction is most evident (**Plate 4.b**).

Impasto arising from the brushwork is indicative of a fluid application of paint, with distinct build-up along edges of colour areas. Where paint has been applied especially thickly, there has been accompanying canvas distortion: this may be seen for example in the leaves of the tree, upper left, and in the collar of the seated woman (**Plate 4.b**).

B.3.iii Short-wave infrared (SWIR)

The interest in technologies capable of imaging artworks past the red end of the visible spectrum, in the ‘near’ (‘NIR’) or short-wave (‘SWIR’) infrared regions, has primarily developed out of the long-standing application to reflectography, exploiting the phenomenon of variable transparency of paint films at different wavelengths to enable visualisation of features lying beneath the surface. Imaging of underdrawing has been a major contribution to the study of authorship in paintings, permitting a fuller comprehension of artists’ working practices and extending the evidence used in attribution questions. Practical experience (as well as theoretical consideration) has shown that deeper IR cameras can confer additional benefits in terms of penetration to underlying layers; consequently, a system capable of operating in the SWIR region was used here (see **Protocol 3.4**).

Due to the fragmentary aspect of the underdrawing, which seems to be rendered in charcoal (see Sample [3], **Plate 17**), only small glimpses of this preparatory stage could be resolved in the SWIR (**Plates 7, 8**) though a general presence of charcoal fragments was observed over the canvas and other exposed areas of ground throughout the painting when examined with magnification (**Plates 13.a, 13.b**). The reason for the lack of resolution in IR lies in a number of factors, probably a combination of the thin and diffuse distribution of the material and the IR blocking properties of the thick overlying layers of paint.

B.3.iv X-radiography and weave analysis

X-radiography shows internal structures in paintings because the transmitted X-rays are blocked to different degrees by virtue of the inherent absorption and thickness variations of the constituent materials. For example, pigments based on lead (such as ‘lead white’) stop the passage of X-rays more effectively than materials based on organic compounds (such as

carbon blacks or the binding medium of the paint), while a thicker application of a material will block more than a thinner one. This allows visualisation of sub-surface features, such as abandoned or altered earlier phases (*pentimenti*), use of techniques such as superimposed forms as opposed to forms left in reserve, characteristic brushwork and so forth.

Here, the prepared surface of the canvas is largely covered by the application of paint, which extends to and over the tacking margins (the size of the painting was reduced slightly, discussed further, below), although small areas of ground are visible throughout the painting where forms abut. Consequently, the X-ray (**Protocol 3.6; Plates 9, 15.a**) reveals a very direct rendition of form, with areas painted in reserve imaging brightly (where they block the passage of X-ray energy), and areas immediately around many of these forms appearing dark. The dark areas in the X-ray corresponding to the thinly primed areas of canvas that were left visible (that is, unpainted; these are more X-ray transparent than the heavily worked regions).

Infilling of the interstices of the threads comprising the canvas support with the priming (ground) and paint also allows the canvas weave to be visualised in the X-ray. Even if a painting is lined, making direct access to the original canvas difficult or impossible, X-ray images can permit the primary weave structure to be examined in detail. A common characterisation of canvases (apart from weave type) is the ‘thread count’, or number of threads per unit in warp and weft directions. Conventionally determined by hand-measuring a number of representative areas, this is now done by applying an image processing algorithm to the entire X-ray image, which has the benefit of providing both greatly enhanced determination of thread counts as well as density and thread orientation information across the whole painting (see **Protocol 3.7; Plates 10.a-d**).

Here, the canvas was found to be a plain weave. The thread count on this work was determined 16.5 threads per centimetre in the vertical direction and 15.5 in the horizontal (**Plate 10.d**). The irregular distribution of stress in the canvas attests to its condition: the cusping distortion at the bottom edge of the canvas suggests that the format of the work has been reduced more along the top edge. The relative lack of cusping along the sides is probably a result of the greater stress applied along the longer axis of the textile. The horizontal divisions seen in the horizontal coordinate map (**Plate 9.a**) are consistent with the surface deformations noted in the 3D imaging, though here perhaps 5-6, rather than 8 or 9, divisions might be interpreted. This may be due to the painting having been rolled at some point, along the long direction.

C. Sampling and analysis

C.1 Introduction

Samples were taken of the support, ground preparation, paint and varnish layers of the work for analysis by different means in order to determine the range of materials (canvas, pigments, binders and coatings) used in the painting, the nature of the preparation layer and the sequence of layering employed in building up the painting.

To this end, a series of 15 locations selected over a representative range of the painting were micro-sampled for identification of the pigments (**Table App.2.i, Plate 16**), with seven micro-samples of paint taken for analysis of the binding media (**Tables App.2.2-2.5**). Two further samples were taken for preparation as cross-sections to study the layering in the selected areas, with the aim of elucidating the development of the painting (**Plates 17, 18**). Finally, canvas threads were taken for fibre identification (**App.2.iv**) and radiocarbon dating (**App.2.v**).

Micro-samples for analysis were taken from locations that were adjudged to be original (that is, were clearly contiguous with those below and adjacent to them, and not retouching or repair). Locations were also further selected to represent as wide a range of the colours – and therefore probably pigments and media – as possible. Thus, the materials identified and discussed below therefore represent, as far as can be determined, the full extent of the original palette used by the artist.

The micro-samples taken for pigment characterisation were subjected to systematic analysis by polarised light microscopy (PLM) combined with UV-visible-near infrared micro-spectrophotometry, scanning electron microscopy-energy dispersive X-ray spectrometry (SEM-EDX) and Raman microscopy (**App.2.i**).

Organic components were identified by Fourier Transform Infrared Spectroscopy-Attenuated Total Reflectance (FTIR; **App.2.ii**) and subsequently by Gas Chromatography-Mass Spectrometry (GCMS; **App.2.iii**).

All of the analytical techniques applied are standard methods within the field, capable of allowing the kinds of differentiation required for this type of work. Comparison was also made between samples from the painting and examples of similar pigments from a large collection of reference standards previously analysed by multiple means⁷. Certain differentiations cannot necessarily be made from this range of techniques, although for present purposes the level of discrimination is thought to be largely or wholly sufficient. All materials were generally identified through a combination of the techniques applied; however, certain key diagnostic features were specifically determined through one or other method.

C.2 Support

The canvas was identified as being based on linen (*Linum usitatissimum* L.) in both warp and weft directions (**App.2.iv; Protocol 2.7**).

C.3 Radiocarbon dating

Radiocarbon dating was applied to fibres from the canvas support.

⁷ The pigment reference collection belongs to the Pigmentum Project (see: <http://pigmentum.org>) and runs to around 3500 samples of both historical and modern origin. Analysis of this collection includes PLM and SEM-EDX as well as other techniques such as X-ray diffraction and Raman microscopy. Access to this research collection is gratefully acknowledged. Reference to specific specimens in the text of this report is to the Pigmentum collection number [Pxxxx]. An organic binding media reference collection is also held by AA&R; samples in this set are cited as [AARxxx].

The radiocarbon date was determined as 141 years b.p. ± 23 years. After calibration, this yielded a date distribution for which the most relevant period for the origin of the canvas lies between 1910 and 1944 at the 95.4% probability level, pre-dating the so-called ‘bomb-pulse’ period that begins in the mid-1950s (**App.2.v; Protocol 2.8**).

C.4 Ground

The ground (present in the cross-sections prepared from Samples [3] and [9]; **Plates 17 and 18**) was found to be composed primarily of a zinc oxide type white with a minor component of aluminosilicates (clay minerals) (**Table App.2.i; Protocols 2.1, 2.2, 2.3**). The ground is bound in a drying oil (**Table App.2.ii; Protocol 2.4.1**). The presence of the zinc white (luminescent in UV light) can be clearly seen in cross-sections prepared; equally evident is the thin nature of the ground (**Plates 17, 18**).

C.5 Underdrawing

Underdrawing is present in the painting and a sample (Sample [10]) taken for PLM analysis. This indicated that the drawing material is charcoal (**Table App.2.i**). This was further confirmed by examination of the cross-section prepared from Sample [3], where the large, charred wood particles are clearly visible (**Plate 17**).

C.6 Paint layers: Pigments

The following **pigments** (**Tables App.2.i, App.2.ii**) were identified in the paint:

- Zinc oxide (‘zinc white’)
- Lead chromate (‘chrome yellow’)
- Earth pigments, yellow toned, containing goethite (‘yellow ochre’)
- Mercury(II) sulfide (‘vermillion’ red)
- Iron hexacyanoferrate(II) (‘Prussian blue’)
- Ultramarine, synthetic, blue
- Ultramarine, synthetic, violet
- Cobalt aluminium oxide (‘cobalt blue’)
- A form of cobalt zinc oxide (‘Rinmann’s green’)
- A carbon-based black
- Calcium sulfate, gypsum type
- Calcium carbonate, calcite type
- Kaolinite
- Barium sulfate

C.7 Paint layers: Binding media

All samples analysed, including material from both ground and paint layers, indicated the presence of a drying oil by FTIR (**App.2.ii**). Additional analysis using GCMS indicated that linseed, poppy



and walnut (or a mixture of linseed and poppy oils) are present in areas of white, yellow and dark blue paint respectively (**App.2.iii**).

FTIR also indicated the presence of metal soaps, probably of lead and zinc, assumed to be reaction products between pigments and binding medium.

C.8 Stratigraphy

The preparation of cross-sections allowed for examination of the overall stratigraphy and composition of the priming and paint layers.

Sample [3], an orange-yellow from the skirt, contains the white ground layer in one area, and displays the bright green luminescence in UV that is characteristic of zinc oxide. Large, splinter-shaped particles of a carbon-based black (probably a char) are visible to the left of the sample, which comprise the underdrawing. The orange-yellow paint layer contains some large colourless particles as well as particles of underdrawing that have been swept up into the paint.

Sample [9], a dark green from the fence, also contains a small fragment of the ground, again containing particles displaying the characteristics of zinc oxide. Overlying this is a granular, light green layer, followed by a distinct darker blue-green layer.

D. Discussion of the findings

D.1 Support, ground and preparatory work

D.1.i The support

The painting has been executed on a medium weight, plain-weave linen canvas (**App.2.v, Plates 10, 11.a**) with thread counts of 16.5 per cm in the vertical direction and 15.5 per cm in the horizontal direction (see **Plate 10.d**). The weave is quite tight, with only occasional, small interstices observed between the threads, which show a 'z' twist.

The canvas weave includes many slub and irregular threads (**Plates 11.a, 4.b**) in both directions of the weave though these are especially common in the vertical (warp) direction. Occasional bits of linen fibre husk may also be observed, indicating that the plant fibres were not cleaned and homogenized to the highest standards before processing as threads. As both selvages are preserved (right and left) it is possible to state the warp and weft directions with certainty, and to note the width of the canvas, 1400 mm.⁸

Although the painting currently measures 1585 mm in height x 1320 mm in width, this is not its original form, which is noted as 1640 mm x 1310 mm in an inscription on the verso (in

⁸ 140 cm was a standard preindustrial canvas width. Callen, A. *The Art of Impressionism*, Yale University Press: New Haven/London (2000) p. 19.

purple, upper left, orientation from the verso '164 x 131': **Plate 5**)⁹. Given the standard measures use for canvas sizes in France in the late 19th and early 20th centuries, it is likely that the canvas dimensions were initially 1620 mm x 1300 mm, a size known as a 'Portrait' format, figure '100'¹⁰. The presence of paint on the tacking edges, as well as the survival of the crease from the original turn over edge in the bottom tacking margin attests to the adjustment, which occurred before the painting entered the collection of the Museum Ludwig (**Plate 12.a**)¹¹. Given that the inscriptions on the verso of the canvas are bisected by the vertical cross bar of the current stretcher, it seems likely that the original secondary support did not have a vertical element such as this (perhaps only a horizontal cross bar).

The irregular distribution of cusping (variable tension in the support caused by the pulling during stretching) is notable in the map of thread density (**Plate 10.a**), clearly showing a distinct distribution along the bottom edge, but less so along the top. This indicates that the stretching was applied more strongly in the vertical direction.

As the painting has been restretched, no evidence for any original inscriptions or labels present on the verso of the stretcher bars survive; those which are present are of a later date¹².

D.1.ii Priming

The canvas has been primed with a white ground layer (**Plate 12.b**) that was found to be composed primarily of a zinc oxide type white with a minor component of aluminosilicates (clay minerals) bound in oil (**Tables App.2.i, App.2.ii**). The aspect of the ground suggests that it is artist applied, not a prepared canvas. The aspects that speak to this interpretation include the fact that the composition of the ground is virtually pure zinc white (as is typical of the grounds applied by Goncharova), the fact that the ground is extremely thin (**Plates 17, 18**) and that its adhesion to the canvas seems quite poor. There is no evidence of a size layer applied to the canvas; along the tacking edges, the ground is seen to have been largely lost (**Plates 11.b, 11.c**) and where it is still present to some degree, it appears to be very thin (**Plate 12.c**). In gaps in the paint film on the surface of the painting, where the ground and canvas have been left exposed, it would appear that the ground is either very thin, or, has been lost due to poor adhesion with the canvas (**Plates 13.a-c**).

D.1.iii Underdrawing

Examination of the painting under magnification revealed the presence of powdery black material along the outlines of the forms of the composition (**Plates 13.a, 13.b**). This material was judged likely to represent remains of the artist's preparatory drawing and a sample was taken for analysis – Sample [10] – and found to be a charcoal. As charcoal is a friable, dry material, unlike paint, it does not have the advantage of a liquid medium to assist in

⁹ See also Franken (2017b) *op. cit.*

¹⁰ See for example, Callen (2000) *op. cit.* p. 15, fig. 24. No information about import of such materials to Russia was known to the authors.

¹¹ See also Franken (2017b) *op. cit.*

¹² These are described in more detail in Franken (2017a), *op. cit.*

adhering it to the surface. Consequently, the particles are held in place only tenuously; often it may be seen that they have been dragged into the paint as it was applied (see cross section 3, **Plate 17**, in which a large black particle is visible at the lower edge, and several other rounded black particles are visible in the body of the paint layers).

Despite the known presence of an underdrawing and the use of high intensity short-wave IR imaging (SWIR) the underdrawing was not resolved in the IR image (**Plates 7, 8**). This phenomenon has been observed with increasing frequency in recent years as more and more late 19th and early 20th century paintings are studied with imaging techniques previously applied primarily to Old Masters. Careful study of such paintings, combined with IR imaging, has documented the common use of underdrawings in the works of many painters where they had not formerly been recognised; equally, these underdrawings, due to their friable nature (thus, easily disrupted and dragged by the paint when applied) and the nature of early 20th century paint (often based on heavy metals, which may contain pigments that do not transmit IR well, as well as being often applied relatively thickly), have been shown not to resolve in most infrared images¹³. The use of underdrawing in *The Jewish Family*, likewise, does not resolve clearly in infrared imaging; only small passages may be faintly seen (**Plate 8**).

D.2 Paint, pigments and binding media

D.2.i General observations

The condition of the painting is generally quite good, although there has been minor loss and flaking, especially along the edges (most clearly visible in the UV and IR images: **Plates 2, 7**). As noted above, the painting has been mounted on a new stretcher, its original dimensions modified, primarily along the upper and lower edges.

The presence of slubby threads and plant husks in addition to the fibrous surface of the canvas all provide the painter with a textured, irregular surface on which to work. Given the use of wide brushes, evident and vigorous brushstroke and little concern for smooth transitions or blending, these characteristics present a consistent aesthetic.

The painting is unusual in the works by Goncharova examined for this study, as it shows signs of adjustment of the composition (*'pentimenti'*) that are unusual for this painter whose work is usually notable for its sureness of brushwork and spontaneity of application. Through the now somewhat transparent white paint of the upper background, bunches of green leaves, abandoned and painted over, are faintly visible (**Plate 3**) on either side of the mass of yellow leaves that are part of the final version of the work. These may also be seen in the X-ray image (**Plate 9.a**). Another colouristic shift took place in the foreground, which once painted in a rust-red tone, before the artist chose to change the colour to grey (**Plate 11.c**; the red tone may be clearly seen in areas of loss, along the tacking margin).

¹³ This fact was first widely noted in the literature during the investigation of Impressionist paintings in the Wallraf Richartz Museum, Cologne, in 2010, during the course of the investigations for the exhibition *Impressionism: Painting in Light*. The phenomenon of friable underdrawing that does not resolve in IR images was observed in Monet's works.

Two more puzzling aspects are seen in the X-ray image (**Plates 9.a** and, especially, **15.a**): the presence of unexplained strokes in the purple skirt of the standing girl with the plaited hair, and, an adjustment of the head shawl of the seated mother, which has been scraped back with a palette knife (**Plates 14.c, 15.b**). The former, visible as a series of hard edged, diagonal brush strokes are puzzling in the context of the relatively uniform purple tone of the garment, and suggest that this area may have been worked over. Equally, the head shawl, now blue and white, may have been a pale green, as is suggested by traces of this colour (**Plate 14.c**) visible in different regions of the shawl. It is unclear whether the presence of the green tone is an intentional addition, or, whether it represents remains of the colour being scraped back.

In addition to these noted changes, the painting is executed with less impasto and surface variation than is seen in some of Goncharova's other work. The surface is largely smooth, characterised by relatively thin applications of paint, laid in overlapping strokes. Exceptions to this rule include, most notably, the yellow leaves of the tree, upper right (**Plate 14.b**). These, in contrast, are applied in confident strokes of a heavily loaded brush. The white collar on the purple dress is another exception, the white paint has largely been swirled around the holes (showing the purple dress below), apart from those in the upper left, which have been painted in purple over the white (**Plates 4.b, 9.a**).

The large forms of colour, created by a network of brushstrokes, show Goncharova's typical manner of working to a pre-set plan. The boundaries of fields of colour often show small exposed areas of ground, and image darkly in X-ray (**Plate 9.a**)¹⁴. This is seen particularly in the manner in which the eyes are rendered; those of the standing child, left, were worked by painting in the pupils, which show white in the X-ray while the whites of the eyes are dark. In contrast, the eyes of the mother are painted in reverse, with the whites of the eyes thickly painted (thus showing white in the X-ray) while the pupils are darker (due to the use of only a thin layer of black paint). Equally, the lines around her hands are dark and distinct in the X-ray, attesting to the degree to which Goncharova adhered to the forms of the set composition.

The use of an underdrawing must have facilitated this manner of working, with very few overlaps of colour or form. No evidence for complex layering was seen; areas are worked quite directly, with mixing both on the palette, and wet-in-wet directly on the canvas. The colours are bright and intense, the paint strongly opaque, ranging from matte to slightly glossy (**Plates 13, 14**). No use of transparent glazes was observed; the colours remain intense, though the surface aspect is quite matt. The painting does not show evidence of having been varnished, in keeping with the artist's preference for a brightly coloured, rough, matte finish.

D.2.ii Paint: pigment and binding medium

The painting has been rendered in a simple palette consisting of one white (zinc white), two yellow tones (chrome yellow and a yellow ochre), one red (vermilion), one green, three blues (mainly ultramarine with small amounts of Prussian and cobalt blues), a violet (ultramarine violet) and black. The dark brown tones are a mix of the yellow earth colour blended with black.

¹⁴ The use of reserves is very common in Goncharova's work. See Rioux, Aitken and Duval (1998) *op. cit.* pp. 19, 25, 26.

While zinc white was used for the ground, it was found to be mainly pure, with only a small addition of clay minerals, while the zinc white used for the painting proper was found to have a minor component of calcium sulfate and trace elements of both aluminosilicates (clay minerals) and barium sulfate.

The cross-sections prepared confirm the observations made on the surface, and with the various forms of imaging: the paint was for the most part worked freely and directly (**Plates 17, 18**) with simple applications of colour rather than complex layering. Mixing has taken place both on the palette, and on the brush, sometimes wet-in-wet directly on the canvas.

D.2.iii Materials analysis and implications for dating

The painting has been dated to 1912 on stylistic grounds. It is known to have first been exhibited in 1913 and a picture exists from the 1940s, of Goncharova in her studio, standing with the work¹⁵.

The radiocarbon measurement of the canvas gave an origin for it between 1910-1944 at the 95.4% probability level, though pre-dating the so-called ‘bomb-pulse’ period that begins in the mid-1950s. In addition to this a period of 3-5 years typically needs to be allowed for processing into canvas and use by the artist, which remains possible in the pre-1913 range for creation.

Equally, the materials identified in the painting are compatible with the supposed date, although they also continued in use after that time. The findings generally agree well with the data collected in the study of 45 paintings by Goncharova and Larionov in the collection of the Musée national d’art modern, Paris¹⁶.

Other technical characteristics arising from the larger review of the works of Goncharova and Larionov may also contribute to a fuller understanding of the relative dating of this painting in the future.

E. Conclusions

The examination of the painting revealed a work that despite an underdrawing (as seems to have been typical for Goncharova), was created with unusual attention and changes of mind, with shifts of colour and form. This considered change of aspect is reflected in the more subdued handling of paint, which is not as rich in impasto brushwork as are many of Goncharova’s paintings. The results of the examination have not found any evidence that would speak against the proposed date of the work, 1912, though given the radio carbon dating, perhaps somewhat later rather than earlier in the year is most plausible.

¹⁵ Franken (2017b) has found mention of three shows, in Moscow and Petrograd, in that year.

¹⁶ The combination of zinc white ground with lead white paint presents the single exception, in that the authors claim that only zinc white was used throughout the paintings by the two artists. Rioux, Aitken and Duval (1998) *op. cit.* p. 18.



F. Acknowledgements

Art Analysis & Research would like to thank the following people for their contributions:

Museum Ludwig

Dr Yilmaz Dzewior	Director, Museum Ludwig	
Rita Kestring	Deputy Director, Museum Ludwig	
Petra Mandt	Deputy Head of Conservation, Museum Ludwig	Project coordinator Paintings conservator

Project Team, AA&R

Dr Jilleen Nadolny	Principal Investigator	Project management
Dr Nicholas Eastaugh	Chief Scientist	Materials and data analysis
Bhavini Vaghji	Senior Scientist	Materials analysis
Francis Eastaugh	Senior Imaging Engineer	Scientific imaging processing
Dr Joanna Russell	Scientist	Materials analysis

Project Subcontractors

Verena Franken	Freelance paintings conservator, Cologne, Germany	Project coordinator, examination, documentation and archival research
Patrick Schwarz	Rheinisches Bildarchiv Köln, Cologne, Germany	Photographic documentation
Prof. Hans Portsteffen, Andreas Krupa	Department of Conservation, Cologne University of Applied Sciences, Germany	Capture of X-ray data
Xavier Aure-Calvet	Freelance imaging specialist, Bristol, UK	3D imaging capture and post processing
Prof Haida Liang and team	Nottingham Trent University, UK	Hyperspectral imaging
Dr Irka Hadjas and team	ETH/ Swiss Federal Institute of Technology, Zurich, Switzerland	Radiocarbon analysis

We would also like to extend our sincere thanks to the Peter and Irene Ludwig Foundation and to the RARP donors and to its board of trustees, without whose generosity and vision this project would not have been possible.

G. Appendices

Standard protocols used by AA&R in the preparation of this report for sampling, materials analysis and imaging are listed in each subsection below and detailed in the appendices to the global summary report.










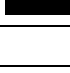
App.1 Sampling and sample preparation

Protocols:

[P.1.1] Sampling









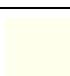
[P.1.2] Cross-sectional analysis

App.1.i Sampling

#	Colour	Description	Location ¹⁷	Analysis
1		White	19/861	PLM, SEM-EDX, Raman, FTIR, GC-MS
2		Yellow	243/1509	PLM, SEM-EDX, Raman, FTIR, GC-MS
3		Orange Yellow	716/0	PLM, SEM-EDX, Raman, FTIR, CSA
4		Brown Yellow	1257/614	PLM, SEM-EDX, Raman
5		Red Orange	482/323	PLM, SEM-EDX, Raman
6		Dark Red Orange (matte)	274/448	PLM, SEM-EDX, Raman, FTIR
7		Dark Blue	0/655	PLM, SEM-EDX, Raman, FTIR, GC-MS
8		Violet	880/212	PLM, SEM-EDX, Raman
9		Dark Green	0/673	PLM, SEM-EDX, Raman, FTIR, CSA
10		Underdrawing	273/454	PLM

¹⁷ The coordinates in this column are given in millimetres, the measurements taken from the left edge of the picture, and from the lower edge of the picture.

Table App.1.i Samples taken for analysis

<i>#</i>	<i>Colour</i>	<i>Description</i>	<i>Location¹⁷</i>	<i>Analysis</i>
11		Dark Brown	125/649	PLM, SEM-EDX, Raman
12		Black	1267/723	PLM, SEM-EDX, Raman
13		Ground	716/0	PLM, SEM-EDX, Raman
14		Black	716/0	PLM, SEM-EDX, Raman
15		Bright Blue	86/242	PLM, SEM-EDX, Raman
16		Canvas fibres	1225/0	
17		Canvas fibre	122/1581	FTIR, C14
18		Canvas fibres for fibre analysis	1225/0	PLM
19		Ground	0/655	FTIR

App.1.ii Cross-sectional analysis

Results are shown in **App.5, Plates 17, 18.**



App.2 Materials analysis summary results

Protocols:

- [P.2.1] Polarised light microscopy (PLM)
- [P.2.2] Scanning electron microscopy and energy dispersive X-ray spectrometry (SEM-EDX)
- [P.2.3] Raman microscopy
- [P.2.4.1] Fourier Transform Infrared Spectroscopy-Attenuated Total Reflectance (FTIR-ATR)
- [P.2.5] Gas Chromatography Mass Spectrometry (GCMS)
- [P.2.7] Fibre Identification
- [P.2.8] Radiocarbon dating

App.2.i SEM-EDX, Raman microscopy and PLM analysis

#	Colour	SEM-EDX (elements)			Raman Microscopy (peaks, cm ⁻¹)	Identification
		Major	Minor	Trace		
1	White	Zn	S, Ca	<i>Al, Si, Cl, Cd, Ba</i>	1007 (vw), 987 (w), 461 (vw), 452 (vw), 437 (vw)	Zinc oxide (main) Calcium sulfate, gypsum type (minor) Barium sulfate (trace)
2	Yellow	Pb	Al, S, Cr	<i>Si, K, Ca, Fe, Zn</i>	972 (vw), 844 (vs), 405 (w), 377 (vw, sh), 361 (s), 337 (vw), 329 (w), 185 (vw), 141 (vw)	Lead chromate [P2238]
3	Orange-yellow	-	Al, S, Ca, Cr, Pb	<i>Si, K, Fe, Zn</i>	839 (vs), 401 (w), 377 (w), 358 (s), 338 (w), 326 (w), 180 (vw), 134 (w)	Lead chromate [P2239] Calcium sulfate
4	Brown-yellow	Si	Al, Fe	<i>Mg, P, S, Cl, K, Ca, Ti, Zn</i>	546 (vw), 399 (vw), 304 (vw), 255 (vw)	Goethite Aluminosilicate clay minerals
5	Red-orange	-	Al, Si, S, Fe, Zn, Hg	<i>K, Ca, Ba</i>	461 (vw), 343 (vw), 285 (vw), 253 (m)	Mercury sulfide Silicon dioxide
					343 (w), 284 (vw), 253 (vs), 140 (vw), 109 (vw)	Mercury sulfide [P0010] Iron containing earth pigments Zinc oxide
6	Dark red orange	Si	Al, Fe	<i>Mg, P, S, K, Ca, Zn, Hg</i>	408 (vw), 343 (vw), 286 (vw), 253 (m)	Goethite Mercury sulfide (trace)
7	Dark blue	-	Na, Al, Si, S, Zn	<i>Mg, K, Ca, Fe, Ba</i>	2155 (vw), 987 (vw), 550 (vw)	Ultramarine Prussian blue (trace) Barium sulfate (trace)
					1580 (vw, br), 1291 (vw, br)	Carbon-based black
					551 (vw)	Ultramarine Zinc oxide
8	Violet	-	Na, Al, Si, S	<i>P, Cl, K, Ca, Zn, Ba</i>	1007 (vw), 546 (vw), 368 (vw)	Ultramarine violet [P0100] Calcium sulfate, gypsum type (trace) Zinc oxide (trace)

Table App.2.i Analytical results SEM-EDX, Raman Microscopy and PLM

#	Colour	SEM-EDX (elements)			Raman Microscopy (peaks, cm ⁻¹)	Identification
		Major	Minor	Trace		
9	Dark green	Zn	Mg	Al, Si, S, Cl, K, Ca, Co	-	Zinc oxide Cobalt zinc oxide (variant) ¹⁸ Cobalt aluminium oxide
10	Underdraw -ing	n.a.	n.a.	n.a.	n.a.	Carbon-based black, as char
11	Dark brown	-	Si, S, Fe, Zn	Al, P, Cl, K, Ca, Mn, Ba	1580 (vw, br), 1286 (vw, br), 1204 (vw), 401 (vw), 300 (vw), 252 (vw)	Goethite Carbon-based black Zinc oxide
12	Black	Ca	P, Zn	Al, Si, S, Cl, Pb	1590 (w, br), 1316 (w, br)	Carbon-based black (bone or ivory black) (main) Zinc oxide (minor)
13	White ground with yellow	Zn	Al, S	Si, Cl, Ca, Cr, Pb	841 (vw), 437 (vw), 401 (vw), 377 (vw), 358 (vw)	Zinc oxide (main) Lead chromate (trace)
					839 (s), 401 (vw), 377 (vw), 359 (w), 338 (vw), 326 (vw), 135 (vw)	Lead chromate [P2239] Clay minerals
14	Black	-	Al, S, Cr, Zn, Pb	Si, Cl, K, Ca, Fe	839 (s), 401 (vw), 377 (vw), 359 (m), 338 (vw), 326 (vw), 134 (vw)	Lead chromate [P2239] Zinc oxide A carbon-based black ¹⁹
15	Bright blue	-	Na, S, Ca, Zn	Al, Si, P, Cl, K, Ba	549 (w)	Ultramarine Zinc oxide Calcium carbonate

¹⁸ This appears to be an unusual variant of cobalt zinc oxide, 'Rinmann's green'. The particle morphology is highly consistent with it being a relatively coarse example of this compound, except that the colour is a pale green-blue rather than the deeper green normally observed. The high levels of magnesium further suggest that this may also be present. A specimen of 'cobalt green' from the Pigmentum Collection, P1300, had similar appearance to the pigment Sample [9] and is known to have an X-ray diffraction pattern close but not wholly corresponding to other specimens of cobalt zinc oxide.

¹⁹ Possibly a char.

App.2.ii Fourier Transform Infrared Spectroscopy-Attenuated Total Reflectance (FTIR-ATR)

Table App.2.ii Summary results from FTIR			
#	Colour	FTIR (peaks, cm ⁻¹)	Identification
1	White	3534 (w), 3399 (w), 3239 (vw), 2955 (vw, sh), 2919 (w), 2850 (w), 1740 (w), 1716 (vw), 1683 (vw), 1618 (m), 1581 (vw, sh), 1574 (vw), 1568 (vw), 1557 (vw), 1541 (m), 1455 (w), 1435 (vw), 1417 (w), 1318 (vw), 1136 (vw, sh), 1110 (vs), 1004 (vw), 983 (vw, sh), 875 (vw), 799 (vw), 723 (vw), 669 (m)	Calcium sulfate, gypsum type [P0026] Calcium carbonate, calcite type Oil ²⁰ Metal soap formation, zinc-based ²¹ Metal soap formation
2	Yellow	3378 (w, br), 2922 (w), 2853 (vw), 1732 (w), 1715 (vw), 1574 (w), 1462 (w), 1412 (vw), 1380 (vw, sh), 1321 (vw), 1157 (vw, sh), 1095 (vw, sh), 1035 (vs), 968 (w), 878 (vw, sh), 851 (vw, sh), 817 (vs), 719 (vw), 683 (vw), 623 (m)	Lead chromate [P2238] ²² Oil Metal soap formation, presumably lead-based
3	Orange-yellow	3524 (vw, sh), 3382 (vw), 3330 (w, br), 2922 (w), 2852 (vw), 1732 (w), 1715 (vw), 1615 (vw), 1575 (w), 1456 (w), 1416 (vw), 1375 (vw), 1319 (vw), 1111 (s), 847 (vs), 812 (w), 666 (vw)	Lead chromate [P2239] Calcium sulfate, gypsum type Oil ²³ Metal soap formation, presumably lead-based
6	Dark red orange	3695 (vw), 3649 (vw), 3620 (vw), 3396 (vw, br), 2951 (vw, sh), 2917 (vw), 2851 (vw), 1729 (vw), 1715 (vw), 1627 (vw), 1456 (vw), 1321 (vw), 1163 (w), 1113 (vw, sh), 1026 (vw, sh), 1001 (vs), 935 (vw), 911 (s), 796 (w), 777 (vw), 754 (vw), 689 (w)	Aluminosilicate clay mineral, kaolinite type Goethite Oil
7	Dark blue	3395 (vw, br), 2954 (vw, sh), 2918 (m), 2849 (w), 1738 (w), 1717 (vw), 1590 (w), 1539 (m), 1456 (w), 1411 (vw), 1398 (vw), 1317 (vw), 1171 (m), 1107 (w), 1069 (vw), 961 (vs), 800 (vw), 780 (vw), 720 (m), 696 (vw), 652 (w), 639 (vw), 608 (w)	Ultramarine Barium sulfate Oil ²⁴ Metal soap formation, zinc-based ²⁵ Metal soap formation

²⁰ The characteristic peak of oil occurring at around 1160 cm⁻¹ was not observed in the spectrum due to the presence of calcium sulfate, gypsum type, whose peaks mask this. However, it is assumed that oil is present due to the formation of metal soaps.

²¹ The peaks present in the sample spectrum matched the reference spectrum of zinc stearate, reference number AAR308. Zinc was identified in the SEM-EDX analysis.

²² The reference spectrum of lead chromate consists of peaks corresponding to lead sulfate. These peaks are also present in the sample spectrum which could suggest that the lead chromate is likely in the form of lead chromate sulfate or lead sulfate is also present in the reference spectrum. The SEM-EDX data of the sample showed high amounts of lead with minor amounts of chromium and sulfur.

²³ As noted 20, above.

²⁴ The characteristic peak of oil occurring at around 1160 cm⁻¹ was not observed in the spectrum due to the presence of barium sulfate whose peaks were masking this characteristic peak of oil. However, it is assumed that oil is present due to the formation of metal soaps.

²⁵ As noted 21, above.



Table App.2.ii Summary results from FTIR			
#	Colour	FTIR (peaks, cm ⁻¹)	Identification
9	Dark green	3397 (w, br), 2953 (vw, sh), 2916 (vs), 2849 (s), 1737 (s), 1716 (w), 1588 (m), 1539 (s), 1462 (m), 1456 (vw), 1413 (vw), 1398 (vw, sh), 1377 (vw), 1320 (vw), 1243 (vw), 1195 (vw, sh), 1167 (w), 1099 (vw), 986 (vw), 742 (vw), 729 (vw, sh), 720 (vw), 668 (vw)	Oil Metal soap formation, zinc-based ²⁶ Metal soap formation
19	Ground from #7 on reverse of the blue	3284 (s, br), 2918 (w), 2851 (w), 1738 (w), 1660 (vw, sh), 1651 (vw), 1644 (vw), 1634 (vw), 1622 (vw), 1615 (vw), 1587 (vw), 1556 (vw), 1548 (vw), 1540 (m), 1454 (w), 1435 (vw), 1415 (vw), 1369 (vw), 1318 (vw), 1237 (vw), 1154 (m), 1103 (vw), 1056 (vw), 1034 (s), 821 (vw), 721 (vw), 667 (vw)	Oil Metal soap formation, zinc-based ²⁷ Cellulose (possibly from canvas fibres)??

App.2.iii Gas Chromatography Mass Spectrometry (GCMS) Analysis

Table App.2.iii Summary results from GCMS					
Sample #	Hexadecanoic acid, methyl ester (C ₁₇ H ₃₄ O ₂)		Octadecanoic acid, methyl ester (C ₁₉ H ₃₈ O ₂)		Ratio
	Retention time, mins	Peak area	Retention time, mins	Peak area	
1	25.655	2.903 x 10 ⁹	29.591	1.506 x 10 ⁹	P/S = 1.93
2	25.663	2.604 x 10 ⁹	29.598	4.607 x 10 ⁸	P/S = 5.65
7	25.665	3.415 x 10 ⁹	29.597	1.155 x 10 ⁹	P/S = 2.96

The P/S value of **Sample [1]**, white paint, was 1.93, consistent with **linseed oil**.

The P/S value of **Sample [2]**, yellow paint, was 5.65, consistent with **poppy oil**.

The P/S value of **Sample [7]**, dark blue paint, was 2.96, consistent with either **walnut oil** or a **mixture of linseed and poppy oils**.

²⁶ As note 21, above.

²⁷ The peaks present in the sample spectrum matched the reference spectrum of zinc stearate, reference number AAR308.

App.2.iv Fibre Identification of the Canvas

Table App.2.iv Canvas fibre identification, Sample [18]		
Sample	Observations under PLM	Interpretation
Warp (vertical)	Nodes across fibres, parallel extinction, s-twist A few structures with low birefringence. One hairy-looking fibre, ribbon-like, bluish-grey in crossed polars	Bast fibre, probably linen (<i>Linum usitatissimum</i> L.)
Weft (horizontal)	Nodes across fibres, parallel extinction, s-twist A few structures with low birefringence, some appearing as broadened ends of fibres – degraded areas?	Bast fibre, probably linen (<i>Linum usitatissimum</i> L.)

App.2.v Radiocarbon measurement

Radiocarbon dating is a method for determining age estimates of formerly living organic materials²⁸. Carbon has three naturally occurring isotopes, ¹²C, ¹³C and ¹⁴C. Both ¹²C and ¹³C are stable, but ¹⁴C decays by very weak beta decay to nitrogen (¹⁴N) with a half-life of approximately 5,730 years. While alive, organic materials continue to exchange carbon with the environment, such that they are in equilibrium. On death, the ¹⁴C component begins to decay, such that over time the relative amount decreases. Measuring the level of ¹⁴C remaining in the material then allows for a date to be estimated. This must be additionally calibrated against natural historical variation in relative ¹⁴C levels in the environment, for which there are accepted standard curves expressing the changes over time²⁹.

Prior to radiocarbon measurement, fibre identification was undertaken and the canvas sample was pre-tested using FTIR to ascertain the presence of any contaminating material that could influence the outcome. As noted elsewhere, the fibre was identified as a bast type, probably linen (*Linum usitatissimum* L.). FTIR indicated the presence of calcium sulfate (gypsum type), and possibly an oil, in addition to the cellulose of the fibre³⁰.

The canvas sample was then submitted to the Laboratory of Ion Beam Physics, ETHZ at the Swiss Federal Institute of Technology (*Eidgenössische Technische Hochschule Zürich*) for radiocarbon dating (see **Protocol 2.7**).

²⁸ Based on from the websites of the NDT Resource Center, <http://www.ndt-ed.org/EducationResources/CommunityCollege/Radiography/Physics/carbondating.htm> and the website of the Oxford Radiocarbon webinfo site: <http://c14.arch.ox.ac.uk/embed.php?File=webinfo.html>, both consulted on 3 February 2013.

²⁹ For example, that used here is one known as IntCal13.

³⁰ Sample pre-treatment aims to remove non-cellulosic materials prior to the radiocarbon measurement.

Table App.2.v.i Radiocarbon measurement										
Sample	Sample	Material	C14 age	$\pm 1\sigma$	F14C	$\pm 1\sigma$	$\delta C13$	$\pm 1\sigma$	mg C	C/N
Nr.	Code		BP				‰			
ETH-77069	AAR0955.D.17	Textile fibre	141	23	0.9826	0.003	-22.8	1	1	401.7

The radiocarbon date was determined as 141 years b.p. ± 23 years. After calibration, this yielded a date distribution for which the most relevant period for the origin of the canvas lies 1910-1944 at the 95.4% probability level, pre-dating the so-called ‘bomb-pulse’ period that begins in the mid-1950s.

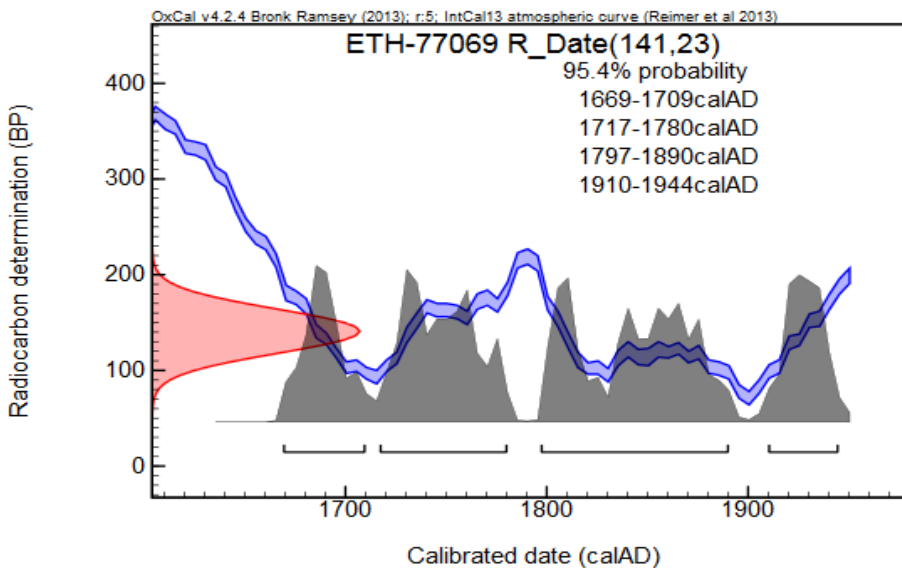


Figure App.2.v.ii
Radiocarbon determination.

App.3 Imaging methods

Protocols:

- [P.3.1] Photography with visible light
- [P.3.2] Photography with ultraviolet illumination
- [P.3.3] 3D laser surface mapping
- [P.3.4] SWIR infrared imaging (IR)
- [P.3.6] X-radiography
- [P.3.7] Thread counting and weave analysis

App.4 Plates



Plate 1. Natalia Goncharova, *The Jewish Family*, 1912, collection Museum Ludwig: Inv. Nr. ML 1369. **Recto, visible light.**

Rheinisches Bildarchiv Köln, Patrick Schwarz, rba_d050886_08, www.kulturelles-erbe-koeln.de/documents/obj/05020007



Plate 2. Natalia Goncharova, *The Jewish Family*, 1912, collection Museum Ludwig: Inv. Nr. ML 1369. **Recto, UV light.**

Rheinisches Bildarchiv Köln, Patrick Schwarz, rba_d050886_06, www.kulturelles-erbe-koeln.de/documents/obj/05020007



Plate 3. Natalia Goncharova, *The Jewish Family*, 1912, collection Museum Ludwig: Inv. Nr. ML 1369. **Recto, raking light.**

Rheinisches Bildarchiv Köln, Patrick Schwarz, rba_d050886_04, www.kulturelles-erbe-koeln.de/documents/obj/05020007

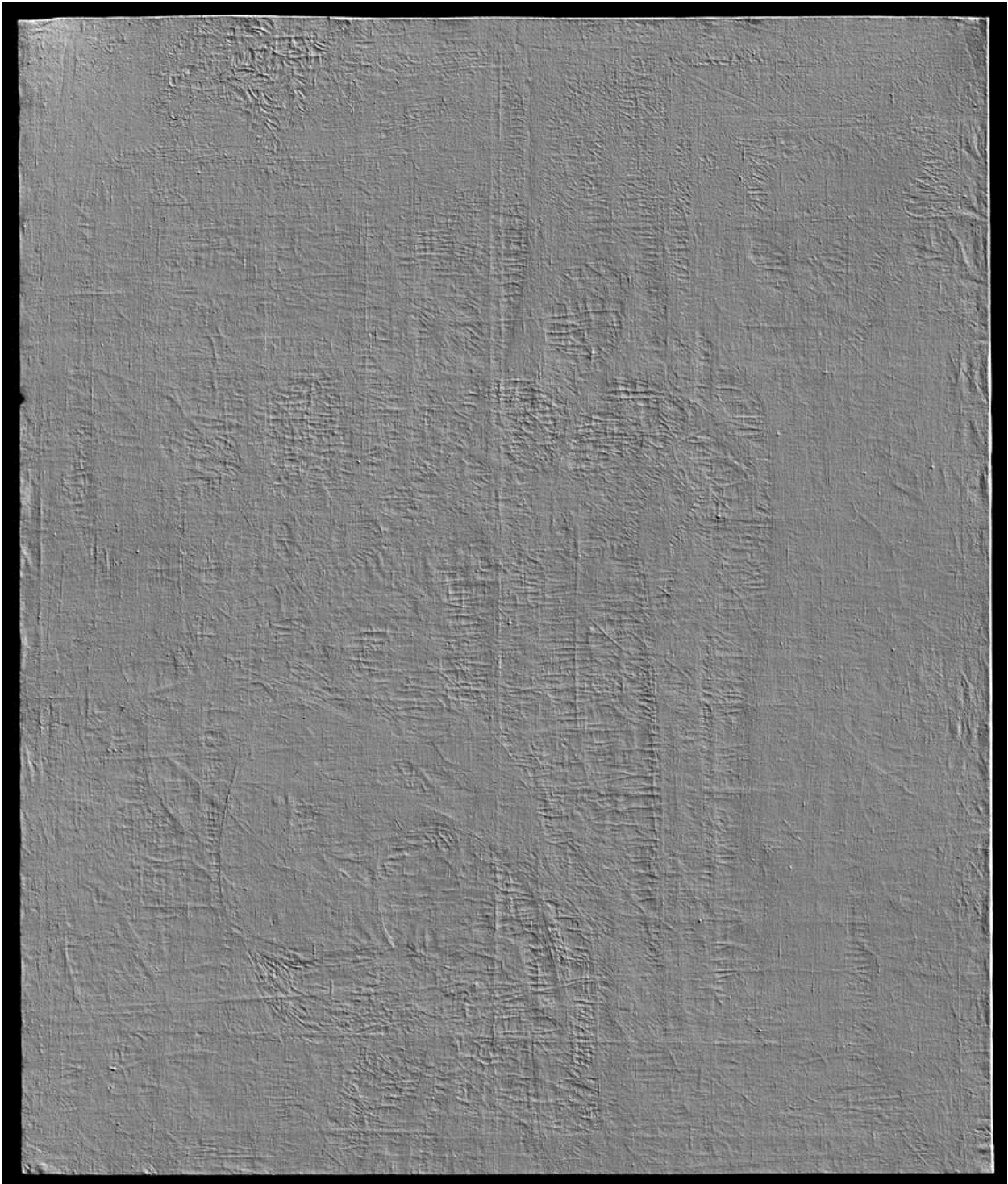


Plate 4.a Natalia Goncharova, *The Jewish Family*, 1912, collection Museum Ludwig: Inv. Nr. ML 1369. **Recto, 3D laser scan.**

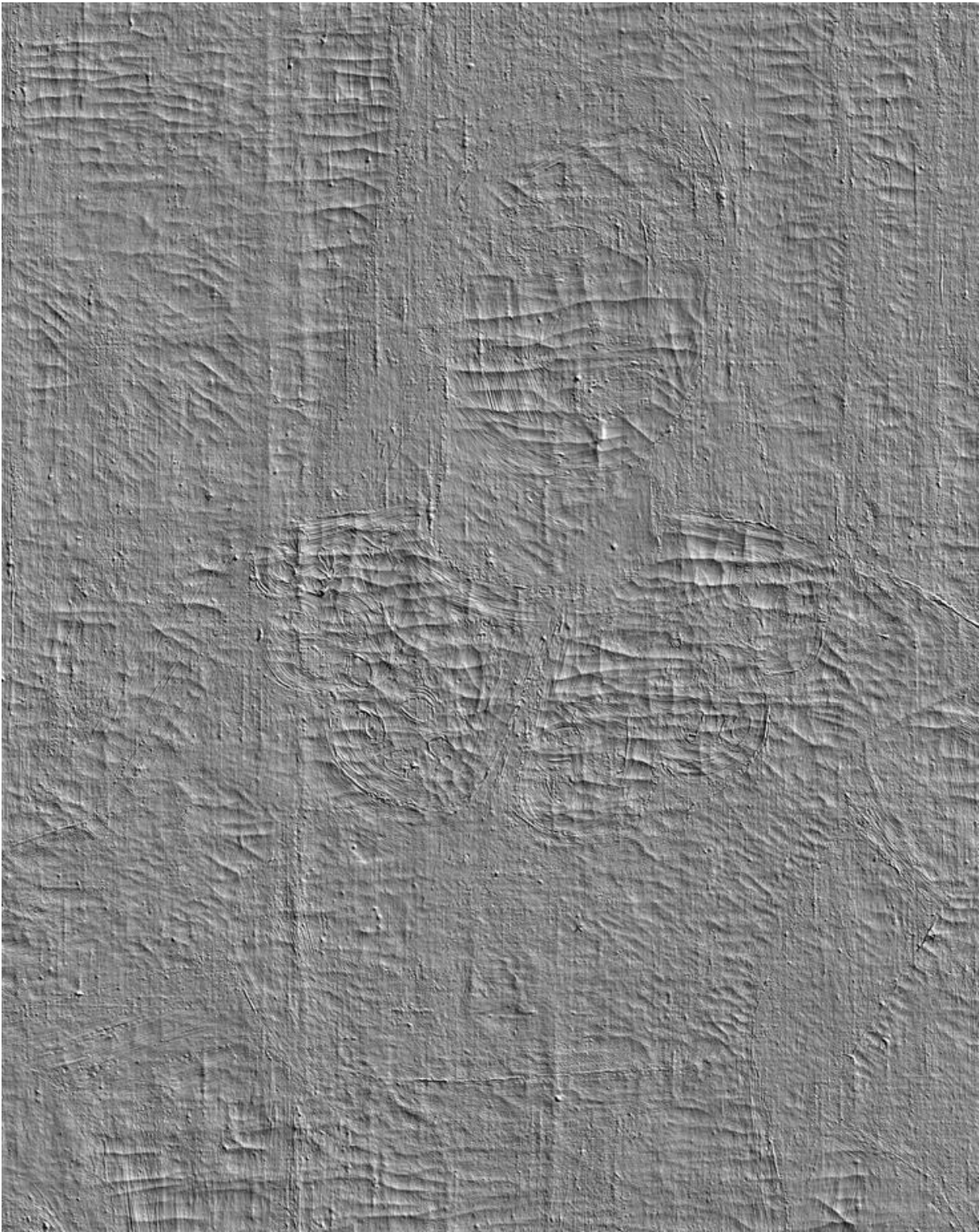


Plate 4.b Recto, 3D laser scan, detail. Figure of the standing woman, face, lace collar, torso.



Plate 5. Natalia Goncharova, *The Jewish Family*, 1912, collection Museum Ludwig: Inv. Nr. ML 1369. **Verso, visible light.**

Rheinisches Bildarchiv Köln, Patrick Schwarz, rba_d050886_02, www.kulturelles-erbe-koeln.de/documents/obj/05020007

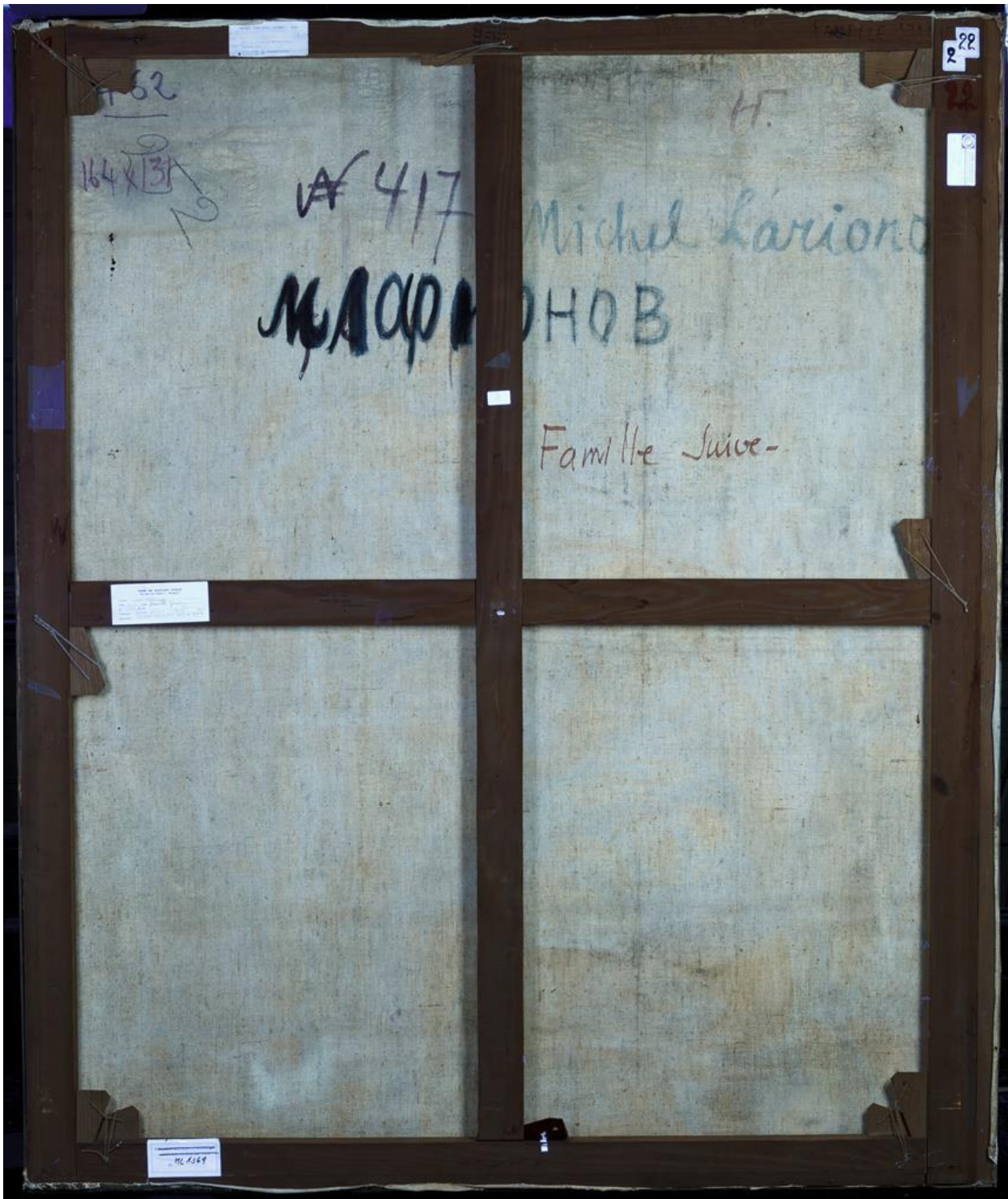


Plate 6. Natalia Goncharova, *The Jewish Family*, 1912, collection Museum Ludwig: Inv. Nr. ML 1369. **Verso, UV light.**

Rheinisches Bildarchiv Köln, Patrick Schwarz, rba_d050886_07, www.kulturelles-erbe-koeln.de/documents/obj/05020007

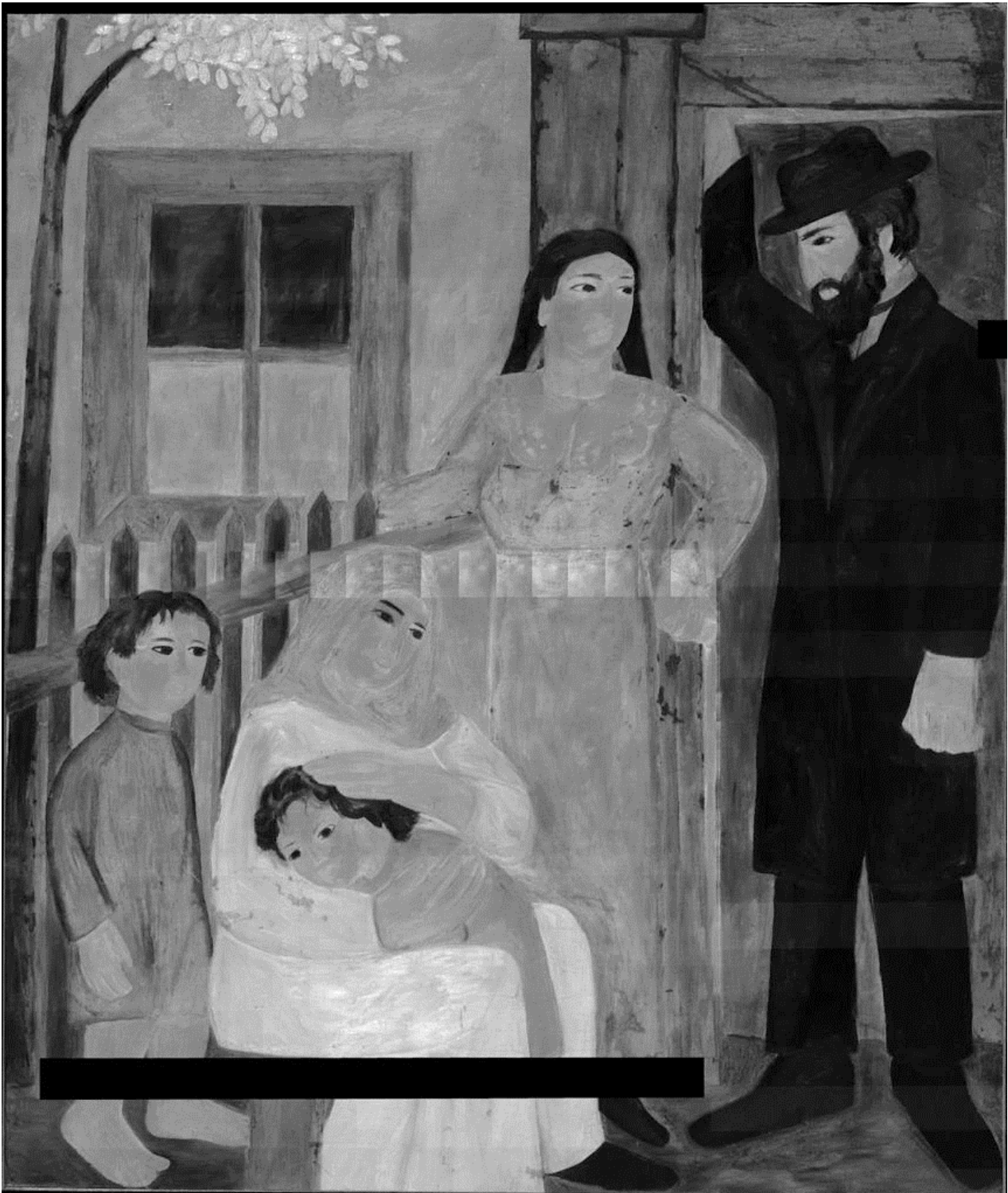


Plate 7. Natalia Goncharova, *The Jewish Family*, 1912, collection Museum Ludwig: Inv. Nr. ML 1369. **Recto, SWIR image.**

The black line, bottom left, is due to lack of information in this region; the banding and grid effects in some areas are due to problems with image capture.



Plate 8. Natalia Goncharova, *The Jewish Family*, 1912, collection Museum Ludwig: Inv. Nr. ML 1369. **Recto, SWIR image, detail.**



Plate 9.a Natalia Goncharova, *The Jewish Family*, 1912, collection Museum Ludwig: Inv. Nr. ML 1369. X-ray image.

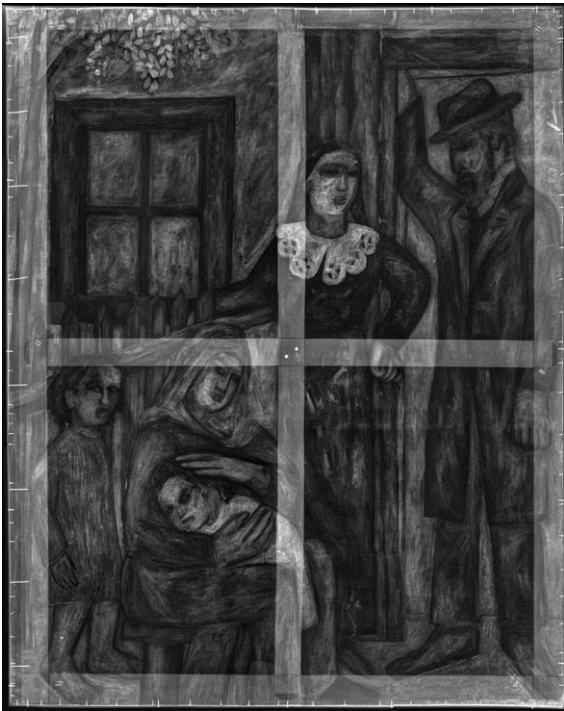


Plate 9.b. X-ray image, before digital compensation for the stretcher bars.

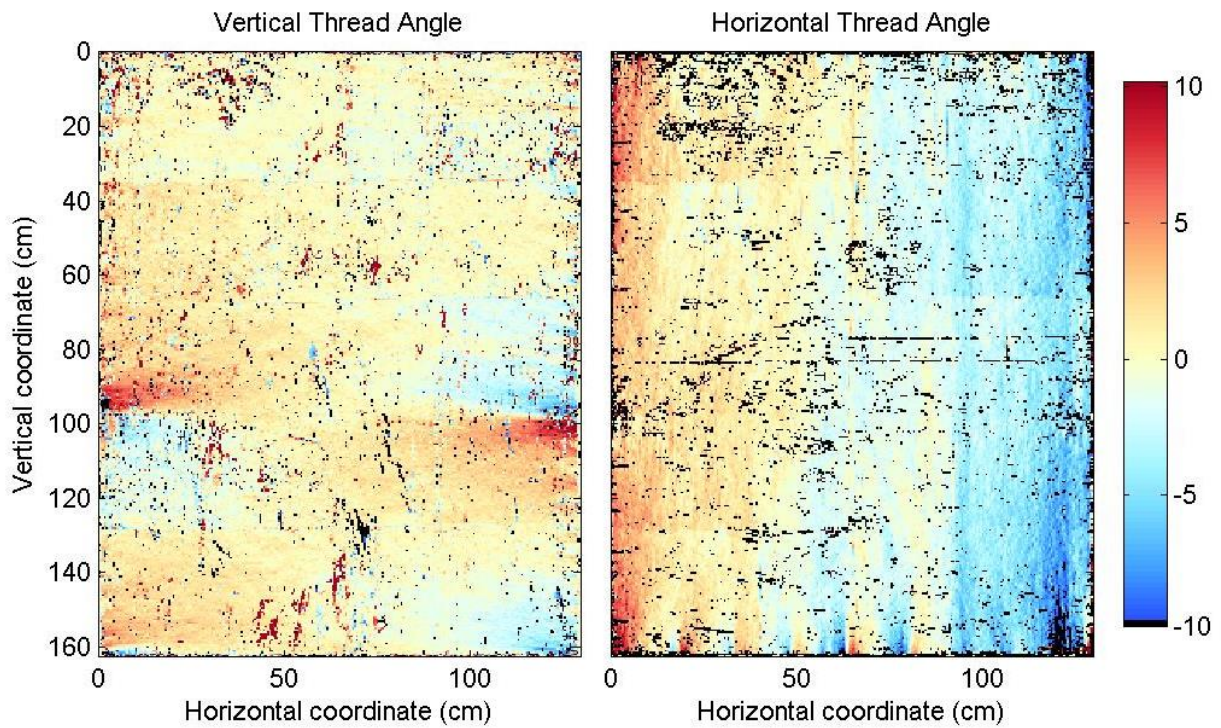


Plate 10.a Maps showing variation in canvas thread angle.

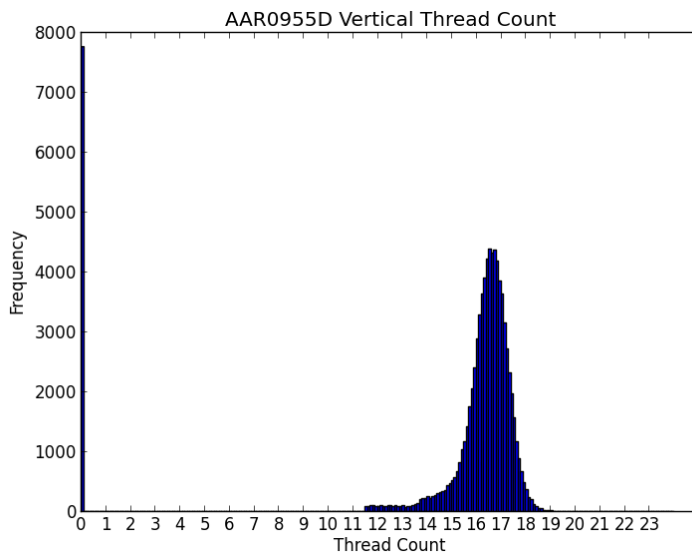


Plate 10.b Histogram of vertical thread count readings.

Showing variation in thread count per centimetre.

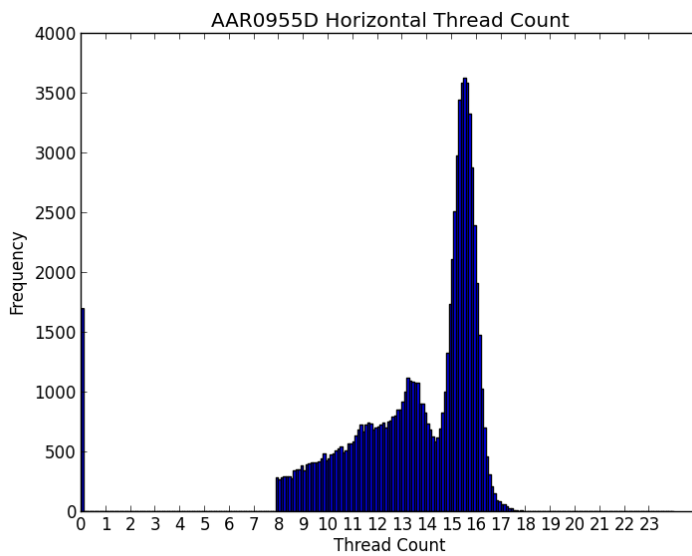


Plate 10.c Histogram of horizontal thread count readings.

Showing variation in thread count per centimetre.

Plate 10.d Table of thread count data (threads per centimetre)		
	Mean	Estimated thread count (mode)
Warp (vertical)	16.41	16.5
Weft (horizontal)	13.73	15.5



Plate 11.a Detail of canvas, verso.

Showing the tight weave of the canvas, with occasional slub inclusions. The fibre is a bast type, probably linen.



Plate 11.b Detail of canvas, left tacking margin, showing selvedge.

The selvedge is preserved along both the right and left sides of the painting.



Plate 11.c Detail of canvas, right tacking margin.

The grey foreground was initially painted in orange-brown. Below, selvage edge.



Plate 12.a Detail of canvas, bottom tacking margin, showing the former turn over edge of the canvas.

The paint surface extends over all four sides, to the largest degree, top and bottom.



Plate 12.b Detail of canvas, left tacking margin, showing loss of white ground.

Plate 12.c (Below) macro detail of the zinc white-based priming on the canvas.

Micro cracking is present in the priming layer.



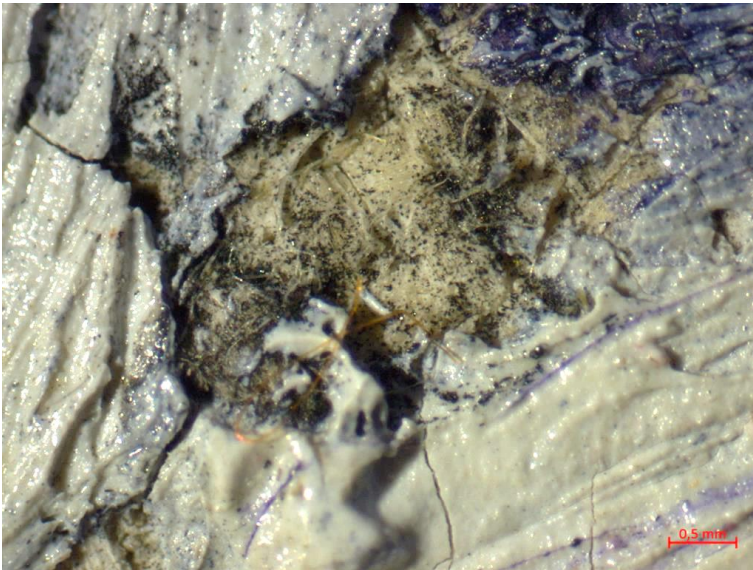


Plate 13.a Detail, recto, showing fibrous surface of the canvas and underdrawing.

The powdery black material is visible where the canvas is not covered.



Plate 13.b Detail, recto, showing canvas and underdrawing.

The fibrous surface of the canvas is exposed, along with some visible traces of ground and underdrawing in an area not covered by paint at the intersection of two differently coloured fields.

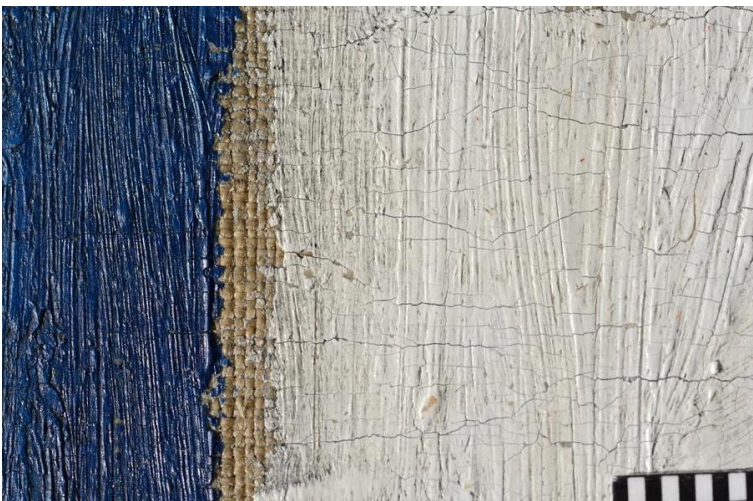


Plate 13.c Detail, recto, showing the exposed canvas with apparent loss of priming.

At the intersection of two differently coloured fields the canvas is exposed, which appears to have lost most of the priming. Brittle cracking of the paint film is also visible.

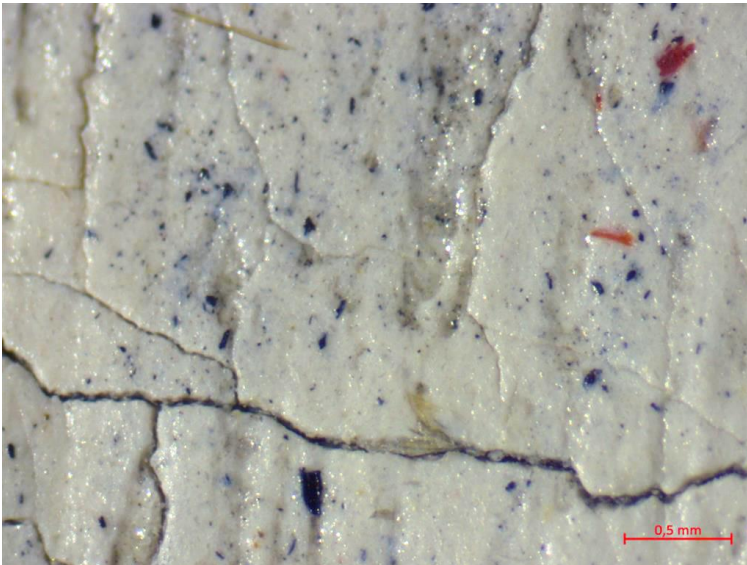


Plate 14.a Microscope detail, showing the large particle size of the pigments.

The paint surface has a flattened aspect.



Plate 14.b Detail, recto, showing brushwork of the leaves.

Formerly, the leaves were painted in green; these were painted over, and replaced by the visible yellow leaves, which are in a different position to the earlier placement. This is visible both in the X-ray, as well as in the visible light image (as the white paint is somewhat transparent).

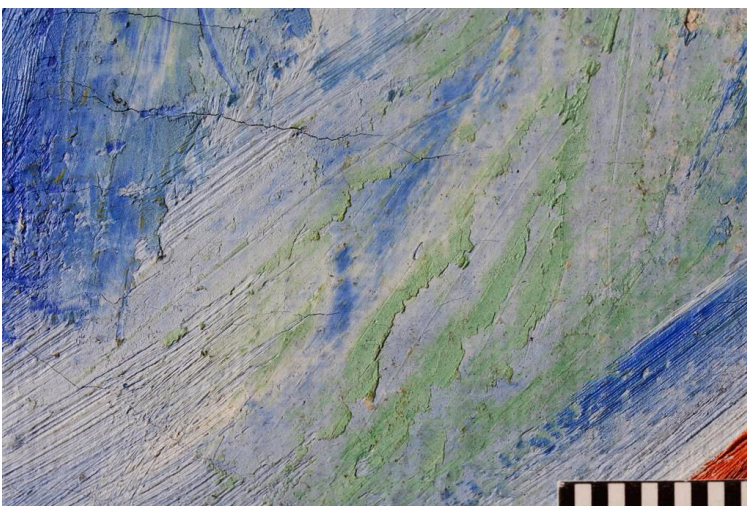


Plate 14.c Detail, recto, showing application of paint with a palette knife.

The surface has been partially scraped down. See Plate 15, below.



a.



b.

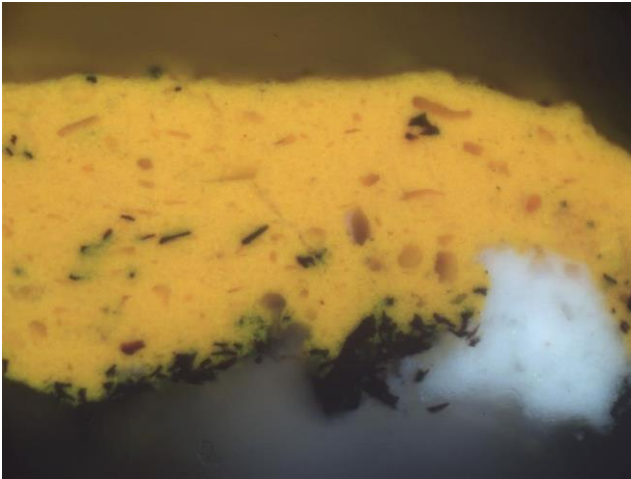
Plate 15. Detail, a.) (above) X-ray.

Left arrow: area of the head scarf that has been scraped back (which shows up as dark). Right arrow: area of the woman's solid purple skirt with unexplained variation in the brushwork (the radio opaque diagonal strokes that show up as white); b.) (left) detail of woman's head scarf, raking light. The whites of the child's eyes are dark in the X-ray as they are not painted, but represented by exposed priming.

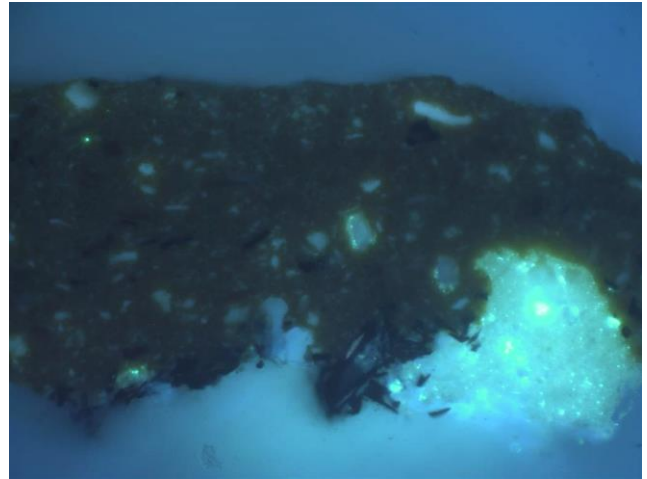


Plate 16. Image showing approximate location of samples taken for materials analysis.

App.5 Cross-sections³¹



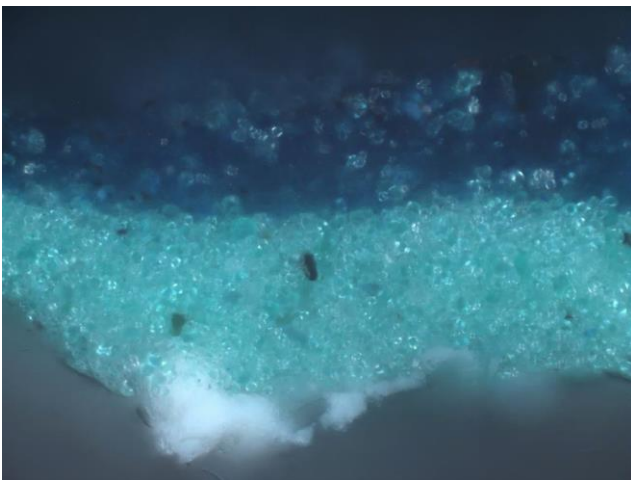
a.



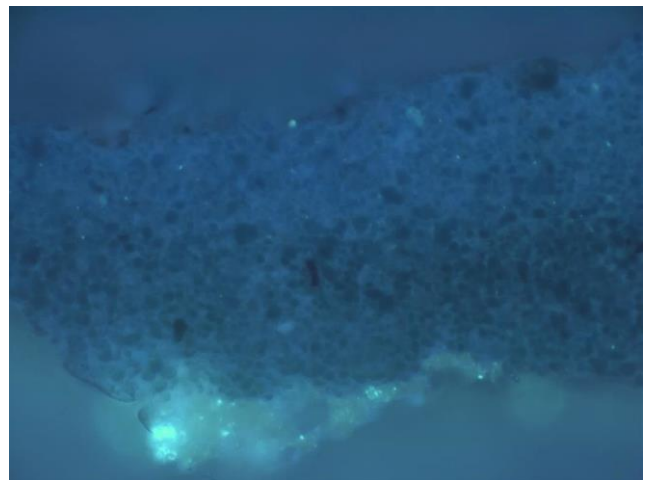
b.

Plate 17. Cross section, Sample [3].

Image ~260µm high. Orange-yellow from skirt. The white ground layer is visible in one area, and displays the bright green luminescence in UV that is characteristic of zinc oxide. Large, splinter-shaped black particles of charcoal are visible to the left of the sample, which comprise the underdrawing. The orange-yellow paint layer contains some large colourless particles as well as particles of underdrawing that have been swept up into the paint.



a.



b.

Plate 18. Cross section, Sample [9].

Image ~260µm high. Dark green from fence. A small fragment of ground is present at the bottom of the sample, again containing particles displaying the characteristics of zinc oxide under UV illumination. This is followed by a granular light green layer, and a darker blue-green layer.

³¹ Photographed under visible light, left (a.), and with ultraviolet illumination, right (b.).